Characterizing the Precipitable Water Vapor of the Atmosphere at Cosmic Microwave Background Observatory Sites

UNM Physics & Astronomy Honors Thesis

Yifu Chen

Advisors: Prof. Darcy Barron

Department of Physics and Astronomy,
University of New Mexico

Date: May 22, 2026

Draft version May 22, 2026
Typeset using LaTeX **default** style in AASTeX7.0.1

ABSTRACT

The Cosmic Microwave Background (CMB) is the first light from the Big Bang, providing fundamental evidence that supports the standard cosmological model. However, ground-based observations of the CMB can be limited by atmospheric water vapor, which varies both over time and across space. We present an analysis of data from a custom scanning Water Vapor Radiometer (WVR), a microwave radiometer that measures atmospheric water vapor. The atmospheric modeling (*am*) package was used to analyze the WVR data. Results include analysis of the impact of parameter changes on the current model atmosphere, including water phases, pressures, and temperatures. To validate our analysis, we compared the processed WVR data with existing datasets, including NASA's MERRA-2 global reanalysis and simultaneous balloon radiosonde flights. The full scanning WVR datasets provide high cadence information about the atmosphere across the entire sky at an observatory site, which can aid CMB data analysis.

Contents

1. INTRODUCTION

This study focuses on how water vapor affects Earth-based millimeter-wave astronomical observations. Water vapor and molecular oxygen strongly absorb specific wavelengths, understanding atmospheric transparency. Because water vapor dominates absorption and emission at these wavelengths, reducing its effects is essential for the high sensitivity required by future Cosmic Microwave Background (CMB) experiments. This project analyzes and validates one year of atmospheric monitoring data from a custom instrument at the South Pole. These methods will be applied to a ten-year dataset from the South Pole, as well as to new data from a second instrument recently deployed at a CMB observatory site in Chile.

1.1. *Background*

1.1.1. *CMB*

The Cosmic Microwave Background (CMB) is fundamental experimental evidence supporting the Standard Model of Cosmology, ΛCDM. According to this model, the early universe was characterized by extreme temperatures and high plasma densities, with photons having sufficient energy to fully ionize hydrogen in the plasma state (S. Dodelson & F. Schmidt 2021). As the universe expanded and cooled, electrons and protons combined to form stable neutral hydrogen atoms during the epoch of recombination. At this stage, photons were no longer strongly scattered by free electrons and began to travel freely through space, forming the relic radiation now observed as the CMB. At the time of recombination, the radiation temperature was approximately 10^4 K, corresponding to a blackbody spectrum that peaked in the ultraviolet. However, its present appearance in the microwave frequency range is a consequence of cosmological redshift.

Since most current and planned CMB observatories are ground-based, atmospheric emission and absorption significantly impact these millimeter-wave observations. Therefore, understanding atmospheric effects, particularly those associated with water vapor, is critical for understanding observational sensitivity and site characterization for future CMB studies.

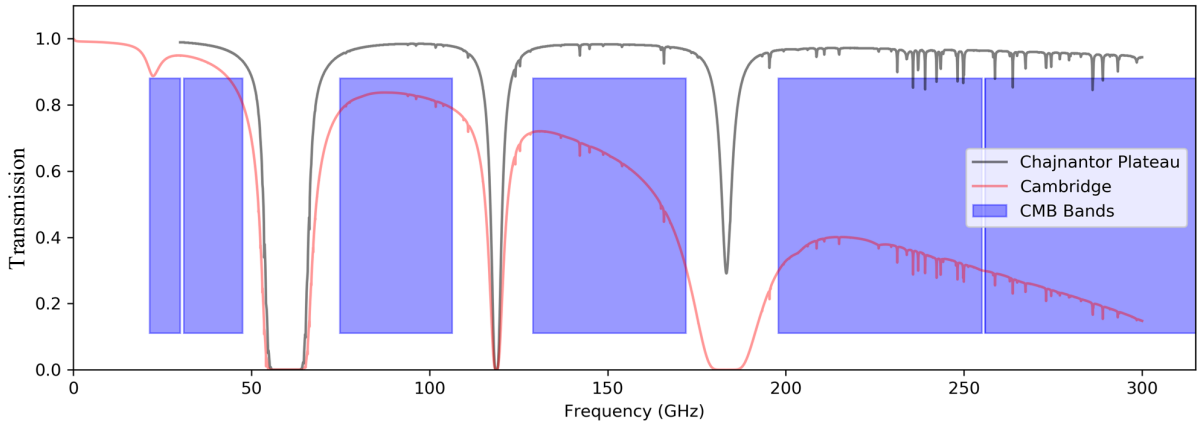

Figure 1. Atmospheric transmission vs. frequency in the mm wavelength, comparing typical conditions in Cambridge, Massachusetts, and the Chajnantor Plateau in Chile. The blue-shaded regions indicate the common CMB observing bands. Figure from Darcy Barron.

1.1.2. *Atmosphere*

The atmosphere's dynamic processes involve the continuous movement and interaction of air, driven by temperature and pressure differences and by the Earth's rotation. Solar radiation exerts a non-uniform heating effect on the planet, thereby inducing pressure gradients that, in turn, give rise to wind systems and large-scale circulation patterns. At smaller scales, atmospheric dynamics encompass a range of phenomena, including turbulence, convection, and the formation of clouds and storms. Concurrently, the Earth's atmosphere influences the transmission of

incoming astronomical radiation across the entire electromagnetic spectrum. Molecules, including water vapor, oxygen, and ozone, absorb and scatter radiation, thereby reducing the sky's transparency at specific wavelengths. In the microwave frequency range, the x-axis of Figure 1 covers the typical CMB observing frequency range, while the y-axis indicates atmospheric transmission, which shows how much incoming radiation can pass through the atmosphere. The blue shaded regions indicate commonly used CMB observing bands, which are designed to avoid strong atmospheric absorption lines. A comparison of typical atmospheric conditions in Cambridge, Massachusetts, and the Chajnantor Plateau in Chile shows the contrast between the two observing sites and the importance of selecting a site with excellent atmospheric properties. The atmospheric spectrum displays specific absorption features attributable to major atmospheric gases. These gases include molecular oxygen, with absorption features observed around 50–70 GHz and 118 GHz, and water vapor, with absorption features observed around 22.2 GHz and 183 GHz.

As shown in Figure 2, the spectral peaks and the continuum come from the emission of these atmospheric gases relative to the much colder background radiation originating beyond the atmosphere. Differences between locations primarily arise from variations in atmospheric temperature and humidity. In tropical regions, higher temperatures and greater water vapor content result in higher atmospheric brightness temperatures. Additionally, lower observing elevation angles increase the path through the atmosphere, which increases the observed brightness temperature. In the millimeter-wave regime, water vapor has the largest effect on sky brightness. Therefore, a comprehensive understanding of water vapor is needed to characterize a given site accurately.

Fig. 1 and Fig. 2 show how the brightness temperature quantifies atmospheric effects differently. At 183 GHz, the transmission decreases and the brightness temperature increases. Precipitable water vapor (PWV) is defined as the integrated amount of water vapor that is contained in a vertical column of air extending from the Earth's surface to the top of the atmosphere, typically expressed as the height of the liquid water equivalent (Murry L. Salby 1996).

As shown in Figure 3, water is not evenly distributed in the atmosphere. At a mid-latitude site in winter, at sea level, the total column of water vapor overhead is about 8.56 mm PWV. At 680 millibars (about 2,800 m), this decreases to about 1.97 mm. At 540 millibars (about 5,200 m), this reaches 0.54 mm. This significant decrease in atmospheric water vapor with increasing altitude is why millimeter-wave observatories are typically located at high-altitude locations. In addition, regions with stable atmospheric conditions, such as the South Pole site, are desirable for large-scale CMB observations.

1.2. *Motivation*

This study aims to develop a method that provides improved water vapor variability and spatial and temporal resolution across different sites.

1.2.1. *Previous Studies*

The study of the atmosphere for various CMB sites has already been conducted using different datasets.C.-L. Kuo (2017) used the Modern-Era Retrospective Analysis for Research and Applications, Version 2 (MERRA-2) datasets. The MERRA-2 data offer information on temperature, pressure, specific humidity, ice and liquid cloud fraction, among other atmospheric parameters. One of the limitations of the MERRA-2 data is the temporal variations, as MERRA-2 only provides two time intervals (1 hour and 3 hours). Also, the spatial resolution of MERRA-2 is about 50 km.

Another study of the atmosphere is the Atacama Pathfinder Experiment (APEX) observatory in Chile. The APEX radiometer has been a long-operating WVR since 2006 (F. Cortés et al. 2020). However, the APEX records data every minute, and the measurement itself has been corrected towards zenith, as described on the APEX webpage [1].

For CMB observations, the spatial and temporal fluctuations of atmospheric water vapor on short timescales produce brightness temperature fluctuations. These atmospheric fluctuations are of particular significance for large angular scale observations. While datasets such as MERRA-2 provide climatological information, they are limited in their ability to capture short-timescale variations in observing elevation angle that directly affect telescope observation or precise site information.

[1] https://archive.eso.org/eso/meteo_apex.html

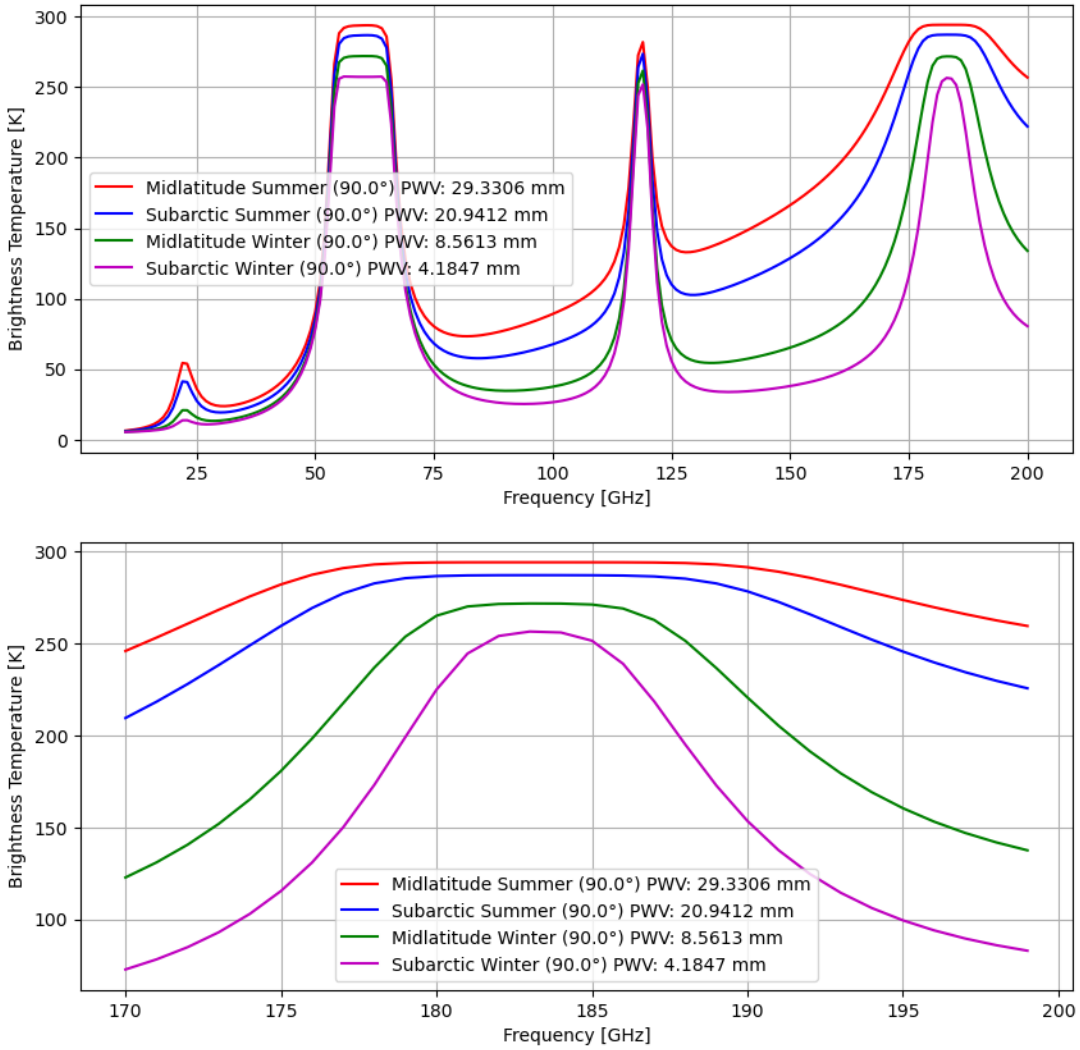

Figure 2. Top: This plot shows the simulation of brightness temperature through the atmosphere and the corresponding spectra computed for two typical climatological conditions: tropical and subarctic winter, at two elevation angles (90° and 30°). PWV is used to represent the amount of water vapor in the atmosphere. Bottom: This plot focuses on the 183 GHz water vapor line. These plot were generated using the PyRTlib package developed by S. Larosa et al. (2024).

2. METHOD

2.1. *Instruments*

Atmospheric dynamics can be measured using radiosondes, instruments specifically designed to measure in situ conditions in the atmosphere. Radiosondes are transported via weather balloons and transmit data to ground stations via radio signals as they ascend through the atmosphere. These measurements generally encompass parameters such as pressure, temperature, and relative humidity as a function of altitude, with altitudes reaching up to 30 kilometers.

A water vapor radiometer (WVR) is designed to measure the quantity of water vapor present within the atmosphere. Here, we focus on WVR targeting the 183 GHz water vapor absorption line. The strength of this spectral line exhibits a high degree of sensitivity to the column density of water vapor. Consequently, WVR measurements at frequencies near 183 GHz (see Fig. 4) provide a direct probe of precipitable water vapor (PWV).

2.1.1. *The Custom WVR*

A custom WVR was developed for CMB atmosphere characterization studies. It can rotate about the azimuth and elevation using two separate step motors and includes an environmental enclosure system that enables it to operate in extremely cold and windy conditions (D. Barkats et al. 2018). Following the scanning strategy of a CMB telescope,

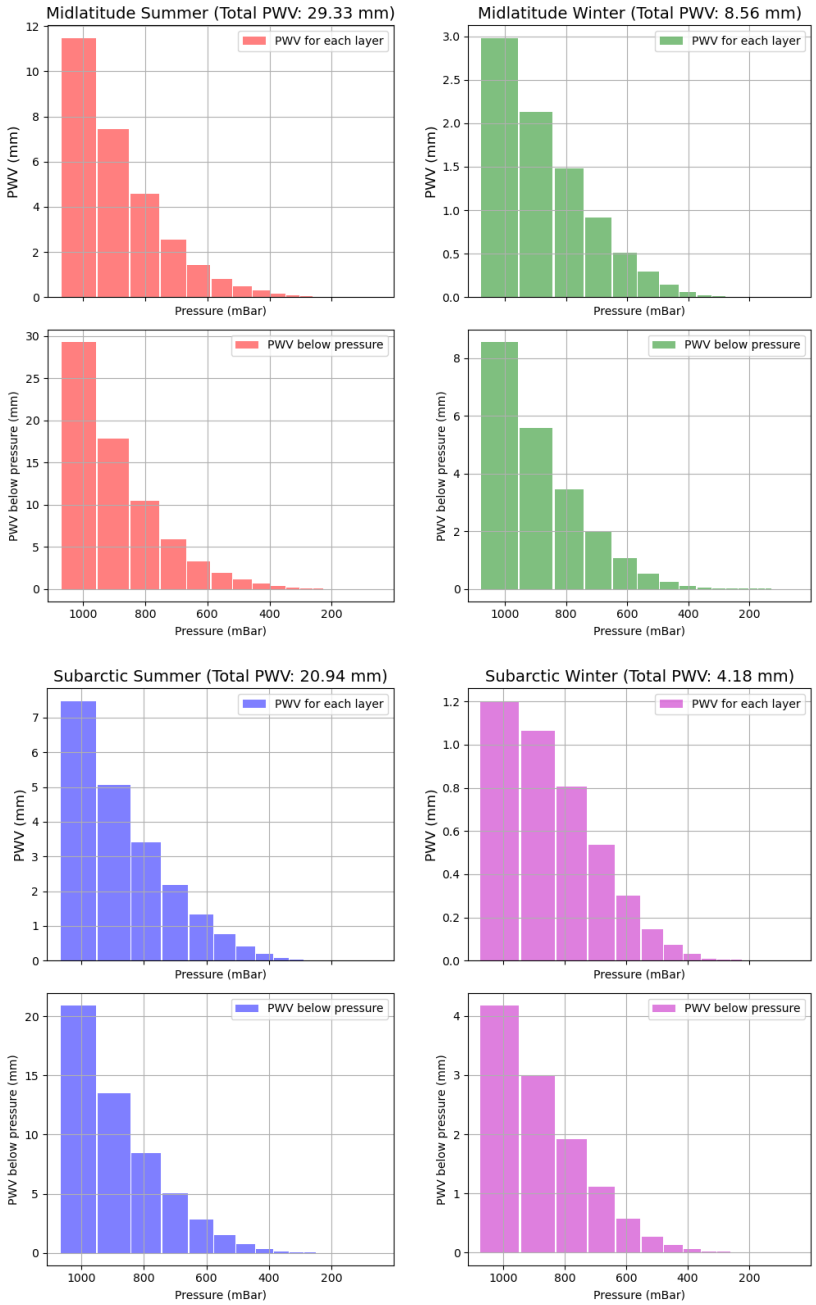

Figure 3. The plots show that the water vapor in the atmosphere is distributed with height. The left top is mid-latitude summer, the right top is mid-latitude winter, the left bottom is subarctic summer, and the right bottom is subarctic winter. For each climatological plot, the top plot shows the water vapor in each pressure layer, while the bottom plot shows the water vapor above the specified height.

the WVR was set to a fixed elevation of 55° when rotating around the azimuth (360°). The beam full width at half maximum (FWHM) is 8°, and the scan is conducted at 2 RPM to freeze atmospheric fluctuations. Furthermore, this custom WVR takes hourly measurements of zenith temperature and opacity. Measurements are taken looking at a hot load, a cold load, and two sky positions to obtain the absolute brightness temperatures. This custom WVR has been installed and operational for about 10 years at the South Pole and in Chile for years. In contrast to previous instruments, this custom WVR enables direct, one-to-one comparisons between different CMB sites by employing identical instruments and measurement strategies.

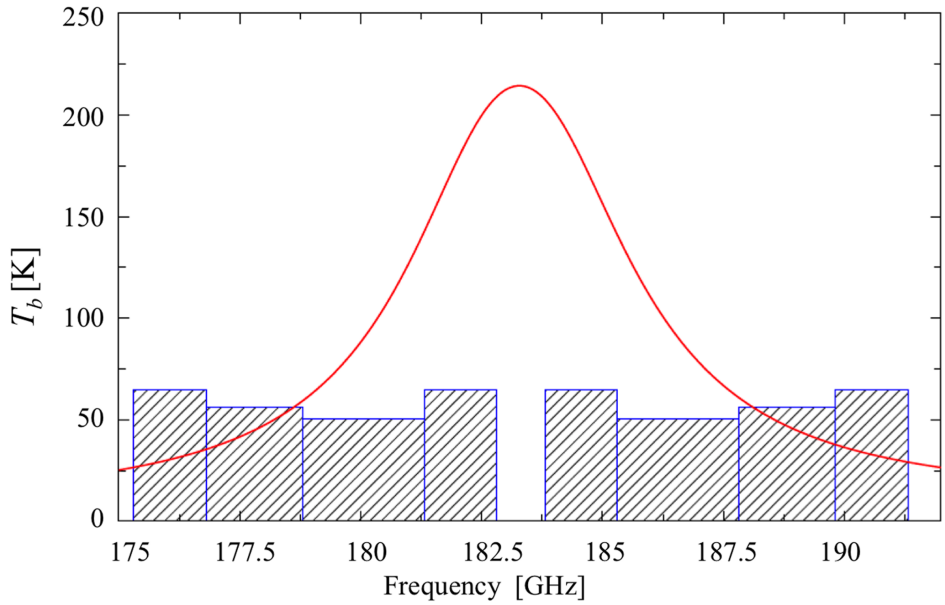

Figure 4. The WVR measures brightness temperatures using four frequency channels centered around 183 GHz. The red curve shows the brightness temperature spectrum of the atmosphere. The shaded blue regions show the bandwidths of the four observing channels used to sample the emission.

2.2. *Data*

A one-year dataset for the custom WVR located at the South Pole was selected for this project to validate the *am* analysis method (detail in section2.3), and includes observation time and brightness temperatures for each channel.

The radiosonde data used in this study were obtained from the University of Wyoming Upper Air Data Archive. Regarding the South Pole station, the launch times are 00:00 and 12:00 UTC. This provides information regarding latitude, temperature, and relative humidity.

2.3. *Analysis Tool (am)*

The atmospheric model (*am*) package is our primary tool for modeling the atmosphere. It is capable of modeling optical depth, radiative transfer, and refraction processes associated with the propagation of electromagnetic waves through the atmosphere and other media, particularly at microwave to sub-millimeter wavelengths (S. Paine 2024). The package offers several features, including computational efficiency, high accuracy, open accessibility, extensive validation, flexibility, and comprehensive documentation. It relies on a detailed configuration format for model specification.

The model includes a built-in capability for performing spectral fits to atmospheric temperature, which we use to derive PWV from our WVR observations. The fitting procedure takes WVR observational data as input and adjusts the parameters within a predefined model configuration file. The resulting output provides the PWV corresponding to the observed atmospheric conditions.

The *am* fit function requires the input of several parameters, including the frequency channels, bandwidths, and measured spectral brightness temperatures. It should be noted that the WVR data file does not contain the frequency and bandwidth parameters, as these values are determined by the instrument setup. The resulting spectral data correspond to the brightness temperatures observed in the four channels (see Fig. 4). The four frequency bands are 0.5–2 GHz, 2–4.5 GHz, 4.5–6.5 GHz, and 6.5–8.5 GHz.

Instead of fitting every second of data, an average brightness temperature was calculated to reduce the number of fits that needed to be performed. To evaluate how temporal averaging affects PWV retrieval accuracy, we analyzed data across several averaging intervals. This approach is predicated on the assumption that atmospheric conditions remain approximately stable over short timescales (on the order of minutes). The mean brightness temperature over a five-minute interval across four channels is displayed in Figure 5.

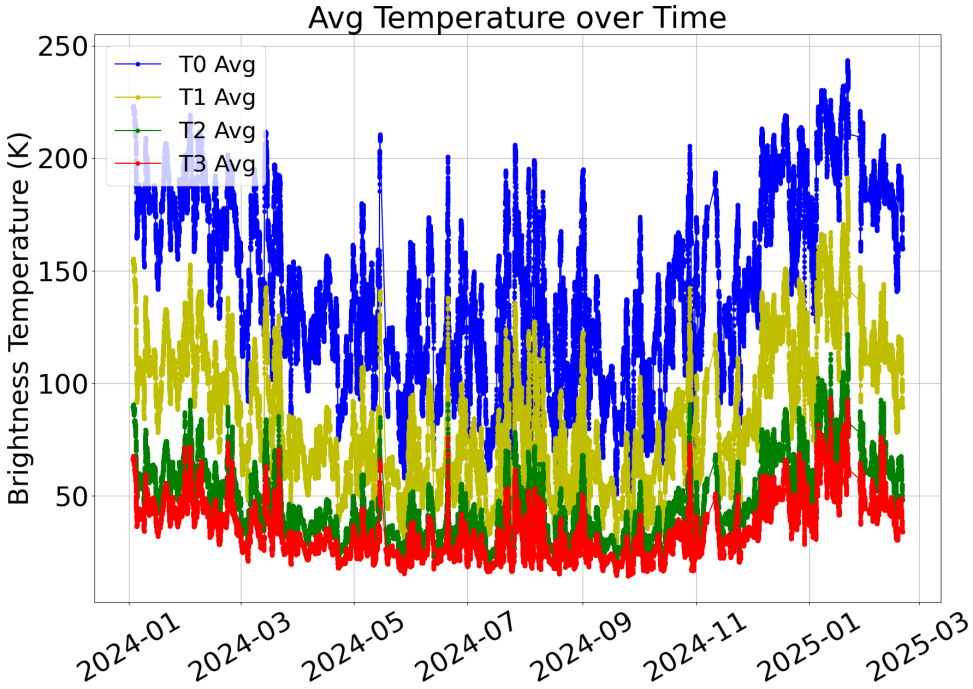

Figure 5. The input signal centered around 183 GHz is separated into four frequency bands: 0.5–2 GHz (T0), 2–4.5 GHz (T1), 4.5–6.5 GHz (T2), and 6.5–8.5 GHz (T3). The WVR measured the average brightness temperature in these four frequency channels from January 2024 to February 2025. Each data point shows the average over a five-minute period.

The *am* model configuration file used in this study corresponds to a standard annual atmospheric profile for the South Pole, incorporating layered atmospheric conditions and initial PWV estimates. During the fitting process, the model adjusts relevant parameters within this configuration to best match the input observational data.

The output file preserves the structure of the atmosphere modeling, while the fitting process provides PWV values for each layer and the total for the atmosphere. A one-year plot of PWV at the South Pole was generated using this method, as shown in Figure 6.

2.3.1. *am Modeling*

To better understand the *am* model configuration file and the subtleties of changing weather conditions, which are especially relevant for the Chile site, we studied variations in water phase and pressure. As shown in Figure 7, the 183 GHz water vapor line varies due to the water vapor becoming water ice in the *am* simulation. For a constant PWV value, an increase in the percentage of water ice results in a decrease in the brightness temperature. This is because water ice typically constitutes a negligible proportion of the total moisture present in an atmospheric column (S. Paine 2024).

As shown in Figure 8, the 183 GHz water vapor line varies due to the change in pressure in the *am* simulation. It has been demonstrated that, for a constant PWV value, a decrease in atmospheric pressure (corresponding to an increase in altitude or changing weather conditions) results in a lower atmospheric brightness temperature. This is what has been discussed in the section 1.1.2.

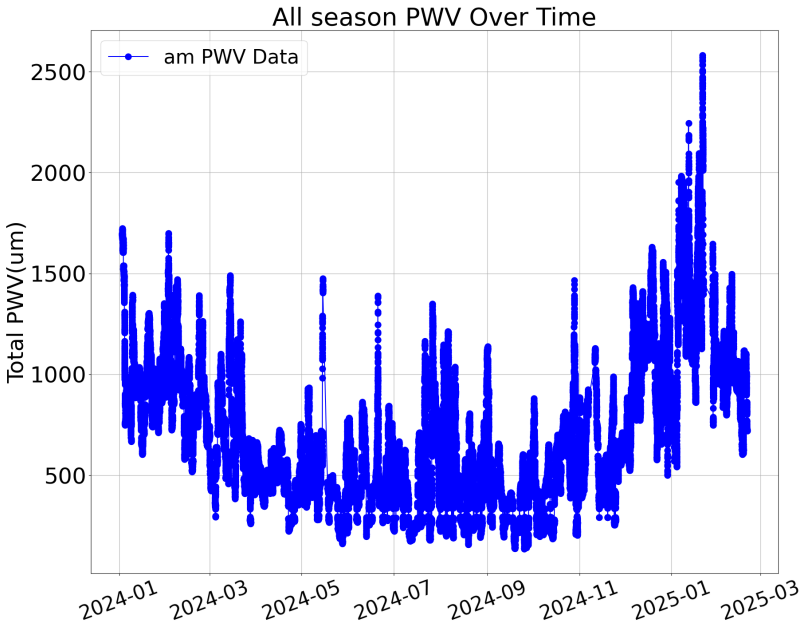

Figure 6. This plot shows the zenith PWV in micrometers (μm) plotted over one year, from January 2024 to February 2025, using the *am* fitting results from the WVR data. The seasonal variation clearly reflects changes in atmospheric water vapor throughout the year.

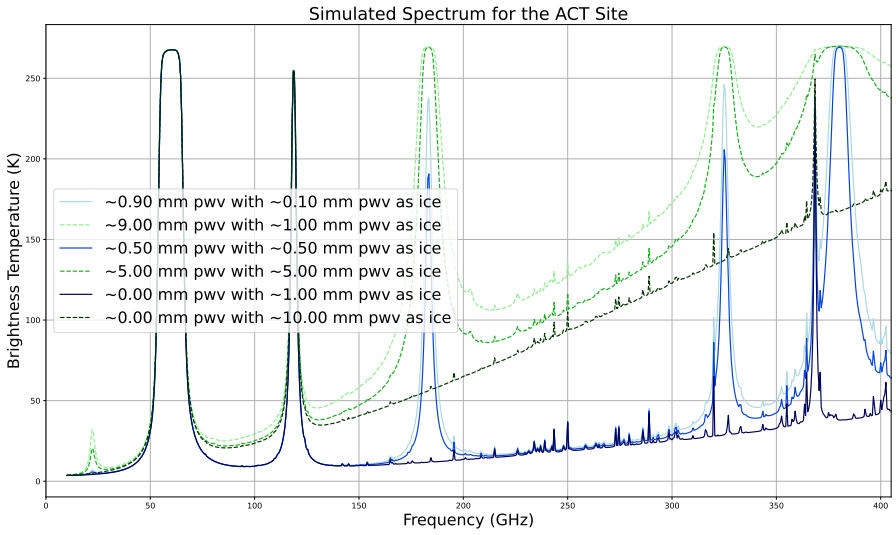

Figure 7. This is the simulation plot of the Atacama Cosmology Telescope (ACT) data in Chile. Simulated atmospheric brightness temperature as a function of frequency for two PWV values: 1 mm (solid lines) and 10 mm (dashed lines). The percentage of water vapor frozen as ice is also varied; lighter colors indicate a lower ice rate, while darker colors indicate a higher ice rate.

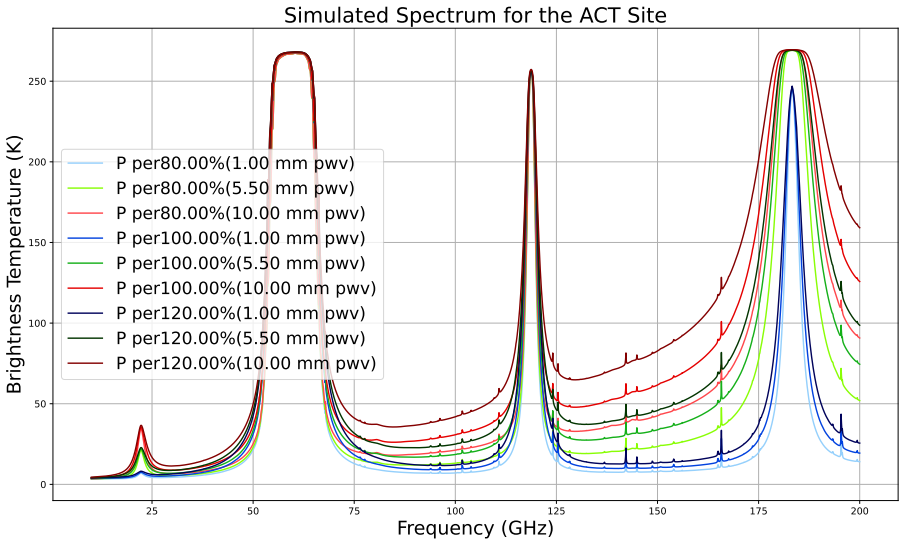

Figure 8. This is the simulation plot of the Atacama Cosmology Telescope (ACT) data in Chile. Simulated brightness temperature spectra showing the effect of varying atmospheric pressure. Each color group represents a different pressure level, while the different line styles correspond to distinct PWV values (1.0, 5.5, and 10.0 mm).

3. RESULTS

3.1. *PWV Distribution*

Preliminary work was conducted using *am* to fit WVR data and convert to PWV, covering a complete year of atmospheric data (January 2024 to February 2025) at the South Pole. The distribution of PWV is shown in Figure 9. From the results, we find a gap where PWV is never around 300 µm PWV, which appears to be an artifact of our simplified modeling and fitting method.

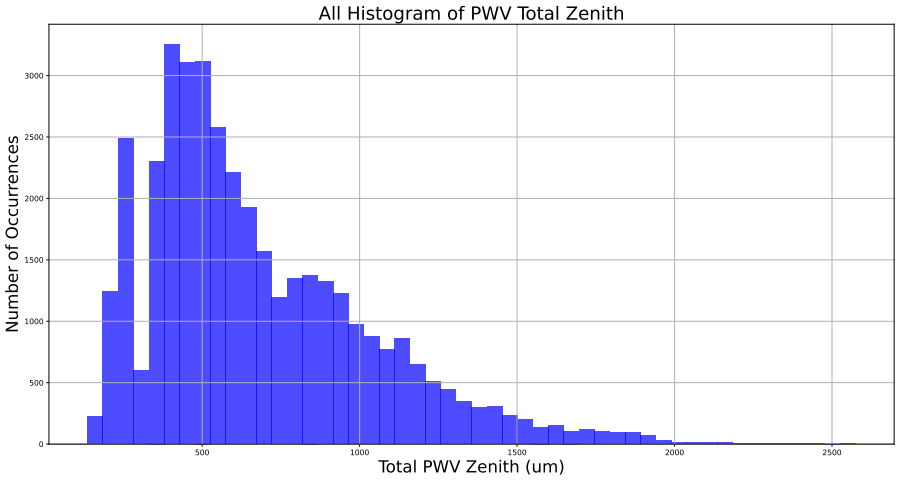

Figure 9. Histogram showing the distribution of PWV values through zenith in micrometers from the full one-year WVR dataset presented in Figure 6.

3.2. *Comparisons*

The MERRA-2 reanalysis results are shown in the upper panel of Figure 10. The MERRA-2 dataset (2014–2016) provides 8-month PWV quartiles of 0.231/0.321 (median)/0.448 mm (C.-L. Kuo 2017), while the *am* fitting (2024-2025) provides the PWV quartiles 0.368/0.471 (median)/0.600 mm. Although a direct comparison is not possible due to the disparate time periods covered by these datasets, the *am* result appears higher in a statistically significant way compared to MERRA-2.

A comparison was made between the results from the data processed with *am* and balloon radiosonde measurements (see Figure 11). While the overall atmospheric structures are consistent, offsets remain between the two measurements. The reason for this offset still needs to be further studied.

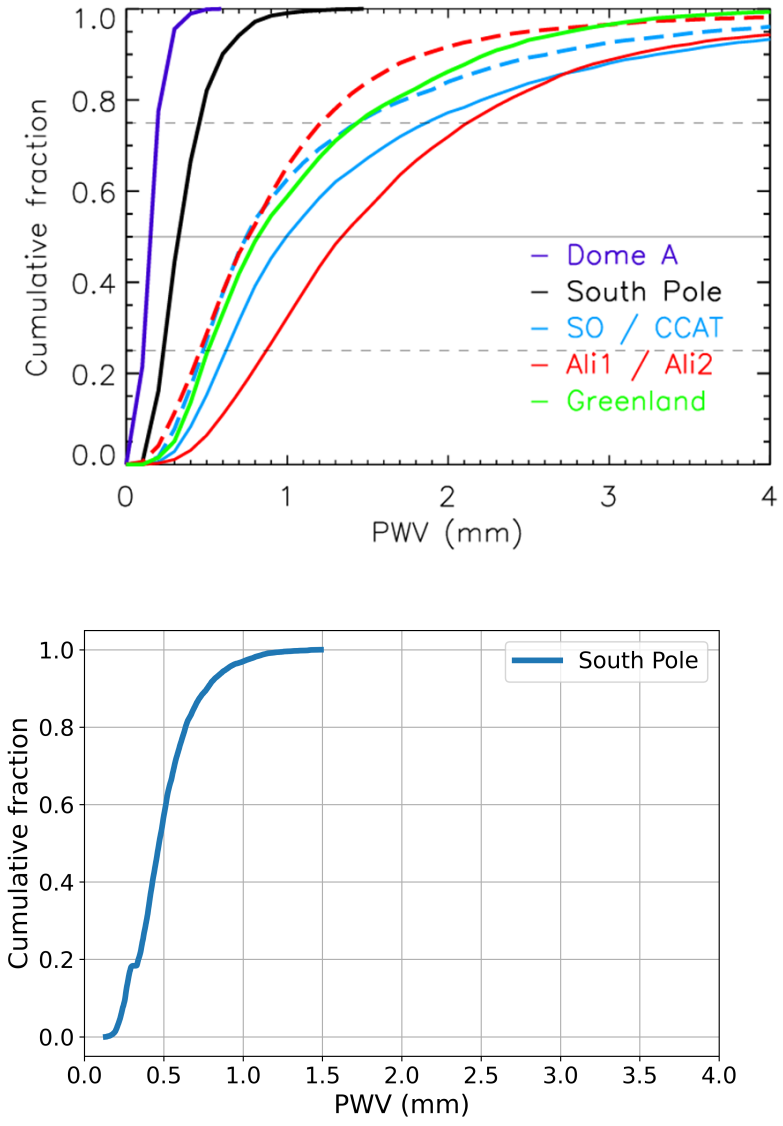

Figure 10. Top: Cumulative distribution of PWV for five mm-wave observatory sites, based on MERRA-2 reanalysis data for the 2014–2016 period. Figure from C.-L. Kuo (2017). Bottom: Cumulative distribution of PWV derived from the *am* fitting results for the South Pole site using WVR data from the 2024–2025 period.

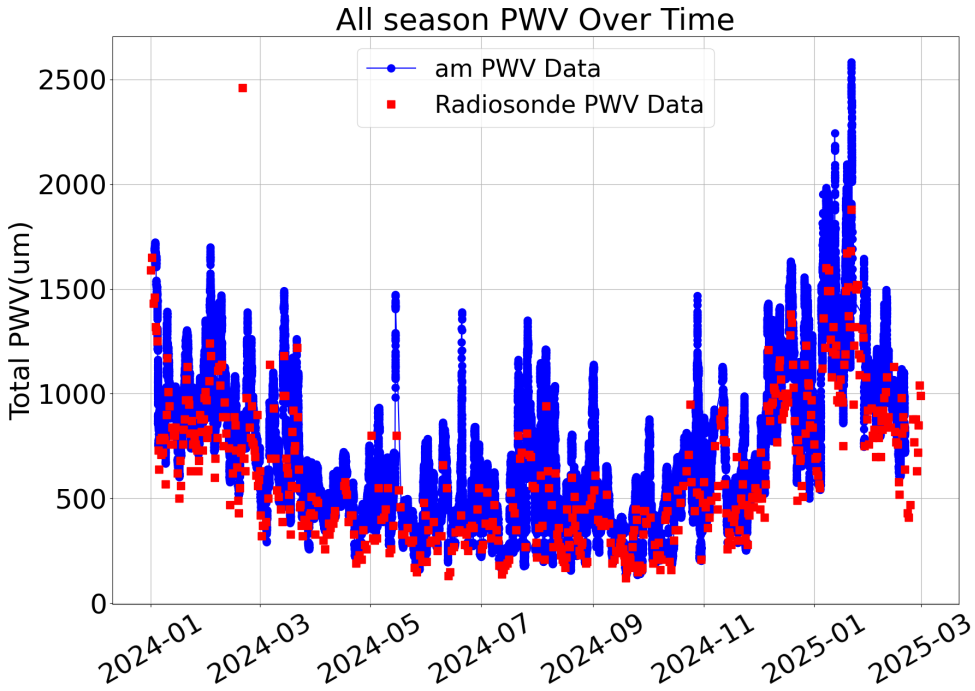

Figure 11. This plot shows the comparison between *am* and radiosonde. The blue points are the same as the top of Fig. 6. The red points show the PWV measured by the radiosonde.

4. CONCLUSION

In this study, the results of the *am* fitting were presented and compared with those of previous studies. This was done to validate our improved PWV measurements for CMB observatory sites. This study contributes to future CMB observations. Despite limitations, this method is a promising tool for improving our understanding of atmospheric conditions at observatory sites and for supporting future studies.

5. ACKNOWLEDGEMENTS

This work was supported by the UNM Physics and Astronomy Rayburn Reaching Up Fund and NSF award 2108704.

I would like to express my deepest gratitude to Dr. Darcy Barron for her invaluable assistance and patient support throughout the duration of this project. I would also like to thank Wilber Dominguez and Tristan Eggenberger for their help in this project. I also acknowledge the team that developed and deployed the custom WVR at the South Pole and Chile: Scott C. Mackey, Alexander Papen, Denis Barkats, Ian Birdwell, Sofia Fatigoni, John M. Kovac, Scott Paine, Matthew A. Petroff, and Abigail Vieregg.

I would like to express my appreciation to my family for their consistent support throughout my academic journey at the University of New Mexico.

REFERENCES

Barkats, D., Bowens-Rubin, R., Clay, W. H., et al. 2018, High-Precision Scanning Water Vapor Radiometers for Cosmic Microwave Background Site Characterization and Comparison, https://arxiv.org/abs/1808.01349

Cortés, F., Cortés, K., Reeves, R., Bustos, R., & Radford, S. 2020, A&A, 640, A126, doi: 10.1051/0004-6361/202037784

Dodelson, S., & Schmidt, F. 2021, in Modern Cosmology (Second Edition), Second edition edn. (Academic Press), 1–19, doi: https://doi.org/10.1016/B978-0-12-815948-4.00007-3

Kuo, C.-L. 2017, The Astrophysical Journal, 848, 64, doi: 10.3847/1538-4357/aa8b74

Larosa, S., Cimini, D., Gallucci, D., Nilo, S. T., & Romano, F. 2024, Geoscientific Model Development, 17, 2053, doi: 10.5194/gmd-17-2053-2024

Murry L. Salby. 1996 in Fundamentals of atmospheric physics, International Geophysics Series No. 61. https://www.sciencedirect.com/bookseries/international-geophysics/vol/61

Paine, S. 2024, The am atmospheric model, https://zenodo.org/records/13748391